Journal of Nuclear Medicine, published on February 9, 2018 as doi:10.2967/jnumed.118.208348

Radionuclide therapy of HER2-expressing human xenografts using an affibody molecule-based PNA-mediated pretargeting: in vivo proof-of-principle.

Running title: Affibody-based pretargeting

Kristina Westerlund*[1], Mohamed Altai*[2], Bogdan Mitran[3], Mark Konijnenberg[4], Maryam Oroujeni[2], Christina Atterby[2], Marion de Jong[4], Anna Orlova[3], Johanna Mattsson[2], Patrick Micke[2], Amelie Eriksson Karlström[1*], Vladimir Tolmachev[2*]

*These authors contributed equally

[1]Department of Protein Science, KTH Royal Institute of Technology, Stockholm, Sweden;
[2]Department of Immunology, Genetics and Pathology, Uppsala University, Uppsala, Sweden;
[3]Division of Molecular Imaging, Department of Medicinal Chemistry, Uppsala University, Uppsala, Sweden;
[4]Department of Radiology and Nuclear Medicine, Erasmus MC, Rotterdam, The Netherlands.

Conflict of interest statement. This research was financially supported by grants from the Swedish Cancer Society, the Swedish Research Council, ProNova VINN Excellence Centre for Protein Technology and the Swedish Agency for Innovation VINNOVA. The authors disclose no potential conflicts of interest.

Corresponding author: Vladimir Tolmachev. Department of Immunology, Genetics and Pathology, Uppsala University, SE-75181, Uppsala, Sweden; e-mail: vladimir.tolmachev@igp.uu.se

First author: Kristina Westerlund, Department of Protein Science, KTH Royal Institute of Technology, Stockholm, Sweden; e-mail: kristina.westerlund@biotech.kth.se

Word count: 4992

ABSTRACT

Affibody molecules are small proteins engineered using a non-antibody scaffold. Radiolabeled affibody molecules are excellent imaging probes, but their application for radionuclide therapy was so far prevented by high renal reabsorption. The aim of this study was to test the hypothesis that affibody-based peptide nucleic acid (PNA)-mediated pretargeted therapy of HER2-expressing cancer extends survival without accompanying renal toxicity. **Methods**. Human epidermal growth factor (HER2)-targeting affibody molecule ligated with AGTCGTGATGTAGTC PNA hybridization probe ($Z_{HER2:342}$-SR-HP1) was used as the primary pretargeting agent. A complementary AGTCGTGATGTAGTC PNA conjugated to the chelator DOTA and labeled with the radionuclide ^{177}Lu (^{177}Lu-HP2) was used as the secondary agent. The influence of different factors on pretargeting was investigated. Experimental radionuclide therapy in mice bearing SKOV-3 xenografts was performed in six cycles separated by 7 days. **Results**. Optimal tumor targeting was achieved when 16 MBq/3.5 μg (0.65 nmol) ^{177}Lu-HP2 was injected 16 h after injection of 100 μg (7.7 nmol) $Z_{HER2:342}$-SR-HP1. The calculated absorbed dose to tumor was 1076 mGy/MBq, while the absorbed dose to the kidneys was 206 mGy/MBq and the absorbed dose to blood (surrogate of bone marrow) was 4 mGy/MBq. Survival of mice in the treatment group (66 d) was significantly ($p<0.05$) longer than survival of mice in control groups treated with the same amount of $Z_{HER2:342}$-SR-HP1 only (37 d), the same amount and activity of ^{177}Lu-HP2 only (32 d), or PBS (37 d). **Conclusion.** The studied pretargeting system can deliver an absorbed dose to tumors appreciably exceeding absorbed doses to critical organs, making affibody-based PNA-mediated pretargeted radionuclide therapy highly attractive.

Keywords: pretargeting, PNA, affibody molecules, radionuclide therapy, HER2.

INTRODUCTION

The concept of pretargeted radionuclide therapy has evolved since late 1980s in response to the limited success of radioimmunotherapy (*1*). Radiolabeled monoclonal antibodies caused an impressive improvement of survival in hematologic malignancies, but failed to deliver therapeutically meaningful absorbed doses to solid tumors without unacceptably high absorbed dose to radiosensitive tissues (*2*). The major problems, i.e. long residence time of antibodies in blood and their inefficient penetration into tumors, are associated with the bulkiness of intact immunoglobulins.

In pretargeting, the process of molecular recognition of tumor-associated antigens is separated from delivery of radionuclide. In a first phase, a primary agent (e.g. an antibody conjugated with a recognition tag) binds to cancer cells and non-bound primary agent then will be cleared from the blood. A small radiolabeled secondary agent with high affinity to the recognition tag on the primary agent is injected thereafter. The small size should ensure rapid penetration into tumor and an efficient renal clearance of free radioconjugate (*3*). Several approaches to pretargeting are under active evaluation (*4*).

For a long time, antibodies were considered as the only class of proteins providing specific high affinity binding. However, non-immunoglobulin engineered scaffold proteins (ESPs) have appeared as a strong complement to or even substitution of antibodies in treatments requiring molecular recognition (*5*). ESP contains a robust scaffold part, which supports variable amino acids. The presence of variable amino acids permits development of extensive combinatorial libraries enabling selection of binders with high specificity to a designated target. The scaffold part reduces entropic penalty and provides very high affinities. Importantly, ESPs can be much

smaller than antibodies, which solves issues of extravasation, homogenous distribution inside tumors, and clearance of unbound targeting agent from the blood (*5*). ESPs, unlike antibodies, can be produced in prokaryotes, which increases appreciably their yield and reduces cost of production, a major advantage for clinical translation (*6*). Several ESPs, e.g. affibody molecules, fibronectins, DARPins, and knottins, have demonstrated promising features as targeting probes for radionuclide molecular imaging (*6*). However, application of many of these ESPs for radionuclide therapy has been complicated due to the high renal reabsorption of proteins after glomerular filtration (*7-10*). We hypothesized that the approach of pretargeting utilizing a secondary hapten with low renal reabsorption might result in safe ESP-based radionuclide therapy. To test this hypothesis we used a human epidermal growth factor receptor 2 (HER2)-targeting affibody molecule as a model.

The scaffold of affibody molecules is based on the 58-amino acid domain B of protein A (*11*). Affibody molecules that bind with high affinity to several cancer-associated targets have been selected (*12*). HER2 is overexpressed in ca. 20% of breast and 15% of gastric cancer and is a predictive biomarker for response to treatment with the HER2-specific monoclonal antibody trastuzumab (*13,14*). The anti-HER2 affibody molecule ABY-025 demonstrated efficient and specific imaging of HER2-expressing breast cancer metastases in clinical studies (*15,16*). Importantly, both preclinical and clinical studies have demonstrated that affibody molecules lack toxicity or immunogenicity. However, the renal uptake of radiometal-labeled affibody molecules was clearly higher than the tumor uptake, which prevented their safe application for radionuclide therapy (*7,15,16*). The renal reabsorption of affibody molecules is megalin-independent (*17*). Conventional methods for reduction of renal uptake of radiopeptides, e.g. co- or pre-injection of cationic amino acids or Gelofusine, were inefficient for affibody molecules (*17*).

Hybridization of complementary peptide nucleic acids (PNA) was selected as one of the approaches to affibody-based pretargeting. PNA is a nucleic acid analog capable of Watson-Crick base pairing (*18*), which can easily be produced by in a good manufacturing practice - compatible way by solid phase peptide synthesis. It is based on an N-(2-aminoethyl)-glycine pseudopeptide chain (**Fig.1A**) instead of a sugar-phosphate backbone, and because of the backbone substitution it is neither degraded by nucleases nor peptidases. PNAs are nontoxic, nonimmunogenic, and capable of hybridization with complementary PNAs in vivo (*19*-*21*). We have developed the complementary PNA hybridization probes HP1 and HP2, conjugated with the chelator DOTA (1,4,7,10-tetraazacyclododecane-1,4,7,10-tetraacetic acid) for radiometal labeling, and established a methodology for site-specific sortase A catalyzed ligation of HP1 to the HER2-targeting affibody molecule $Z_{HER2:342}$, forming the $Z_{HER2:342}$-SR-HP1 affibody-PNA chimera (**Fig. 1B and 1C**) (*22*). $Z_{HER2:342}$-SR-HP1 binds HER2- expressing cells specifically with an affinity of 6±2 pM and radiolabeled HP2 binds to $Z_{HER2:342}$-SR-HP1-pretreated cells with an affinity of ca. 300 pM (*23*). HER2-specific accumulation of ^{111}In-$Z_{HER2:342}$-SR-HP1 and pretargeting-dependent uptake of ^{111}In-HP2 in HER2-expressing xenografts have also been demonstrated (*23*). Importantly, we have found that tumor uptake of ^{111}In-HP2 was twice the renal uptake after pretargeting. Although this difference was insufficient for tumor treatment without damaging kidneys, the renal uptake was already reduced 20-fold compared with non-pretargeted radiometal-labeled affibody molecules, which suggested that a further optimized pretargeting approach might lead to safe and effective affibody-based radionuclide therapy. Moreover, efficient labeling of HP2 with the therapeutic radionuclide ^{177}Lu has been established (*24*).

The aim of this study was to evaluate factors influencing affibody-based ^{177}Lu-HP2 pretargeting and to test the hypothesis that affibody-based pre-targeted therapy can prevent renal toxicity and improve survival of mice bearing HER2-expressing xenografts.

MATERIAL AND METHODS

Targeting Probes

$Z_{HER2:342}$-SR-HP1 and HP2 were produced and purified as described earlier (*22, 24*). Briefly, the PNA hybridization probes, HP1 and HP2, were synthesized using manual Fmoc-protected solid phase synthesis on a Rink-amide ChemMatrix resin using commercially available building blocks. HP1 was covalently and site-specifically ligated to an anti-HER2 affibody using an enzymatic, sortase A mediated ligation. The affibody construct, $Z_{HER2:342}$-SR-H_6, was expressed in E. coli and purified using standard protocols for His_6-tagged proteins prior to ligation. The targeting agent $Z_{HER2:342}$-SR-HP1 and the secondary agent HP2 were both purified on a reversed phase (RP) HPLC column using a water/acetonitrile gradient with 0.1% TFA. The final purity of $Z_{HER2:342}$-SR-HP1 and HP2 used in this study was ≥ 95% as judged by analytical RP-HPLC.

For labeling, a solution of HP2 in 1 M ascorbic acid, pH 5.5, (0.5 μg/μL) was mixed with ^{177}Lu-chloride (4.8 MBq per μg HP2). The mixture was incubated at 95 °C for 60 min and radiochemical purity was measured using radio-ITLC eluted with 0.2 M citric acid, pH 2.0. The purity of $Z_{HER2:342}$-SR-HP1 was over 95%. Secondary probe ^{177}Lu-HP2 was produced and labeled as described (*24*). The radiochemical purity of ^{177}Lu-HP2 was over 98%, and the specific activity was 24.7 GBq/μmol.

Optimization of Pretargeting

Animal experiments were performed in accordance with the national legislation for work with laboratory animals. The ethical approval was granted by the Ethical Committee for Animal Research in Uppsala. Animals were euthanized using Rompun/Ketalar anesthesia.

For biodistribution studies, BALB/C nu/nu mice were subcutaneously implanted with 10^7 HER2-expressing SKOV-3 cells. Experiments were performed 2-3 weeks after implantation of tumors. Influence of co-injection of Gelofusine, molar ratio of primary and secondary probes, time between injection of primary and secondary probes, and possibility of increasing the delivery of ^{177}Lu to tumors were evaluated. Gelofusine is a plasma expander, which reduces the renal re-absorption of many radiopeptides (*25*). It was found that co-injection of Gelofusine reduces renal uptake of ^{177}Lu-HP2 (*24*).

Five mice per data point were used. Animals were injected with a pre-determined amount of $Z_{HER2:342}$-SR-HP1 in the tail vein. After preset time, mice were injected intravenously with 120 kBq ^{177}Lu-HP2 each. The injected HP2 mass was adjusted to the pre-determined amount for each group by adding unlabeled HP2. For details, see **Table 1**. The animals were euthanized one hour post injection (p.i.) of ^{177}Lu-HP2, organs were excised, weighed and their radioactivity was measured using automated gamma-spectrometer (PerkinElmer).

Biodistribution and Dosimetry

To evaluate dosimetry, groups of five mice were injected with 100 µg (7.6 nmol) $Z_{HER2:342}$-SR-HP1, 3 µg (120 kBq) ^{177}Lu-HP2 per mouse was injected 16 h later. Biodistribution was measured at 0.3, 1, 4, 24, 48, 144 and 216 h after ^{177}Lu-HP2 injection, as described above. To evaluate dose to renal cortex, kidneys of two mice were excised 1 h after injection of ^{177}Lu-HP2 (3 µg, 1MBq) and 20 µm-cryosections were prepared. Distribution of radioactivity in the sections was measured by digital autoradiography using a Cyclone Storage Phosphor System (PerkinElmer) (Supplemental Fig.1). Specific S-factors for radioactivity uptake in the renal cortex were determined with a small scale radiation transport calculation in MCNP version 6. The

cortex was modelled as a 1 mm thick rim inside a 4.8 x 5.7 x 9.8 mm ellipsoid. Absorbed doses were calculated with use of the RADAR realistic mouse phantom (*26*). Absorbed doses to the tumor were calculated with the spherical node S-values (*27*) without considering contribution to the tumor absorbed dose from activity in the mouse. The absorbed dose to the spleen could well be considered to be representative for calculating the absorbed dose by activity in the mouse to the tumor placed in the abdomen. When we perform these calculations the absorbed cross-dose to the spleen from other organs is in the order of 8.5 mGy, which would increase the absorbed dose to the tumor by 0.05%. Considering all uncertainties in the absorbed dose calculations this may be considered to be completely negligible. Tumor volumes were taken from data concerning SKOV-3 xenograft growth in untreated control mice form previous studies (Supplemental Fig.2) .

Experimental Therapy

To evaluate pretargeted therapy, 10^7 SKOV-3 cells per mouse were implanted subcutaneously on the abdomen. At least twice a week mice were weighed, visually inspected, and the tumor size was measured using electronic calipers. Tumor volumes were calculated using the formula: tumor volume [mm^3] = (length [mm])×(width [mm])^2×0.5. Animals were euthanized when tumors reached a size of 1000 mm^3 or were ulcerated, or if the animal weight was reduced by more than 10% during one week or more than 15% after the study start. After euthanasia, tumors and kidneys were excised for subsequent histological evaluation

Treatment started 14 days after tumor implantation, when the average tumor volume was 83±43 mm^3. Mice were randomly divided into 4 groups, 10 animals each. Mice in the treatment group were injected with 100 µg (7.6 nmol) $Z_{HER2:342}$-SR-HP1, and 16 h later 3.5 µg (0.65 nmol)/16 MBq ^{177}Lu-HP2 in 100 µL solution containing 2% bovine serum albumin and 4 mg

Gelofusine was injected. Control group 1 was injected with vehicle alone. To evaluate the influence of non-labeled $Z_{HER2:342}$-SR-HP1 on tumor growth, a control group 2 was injected with 100 µg (7.6 nmol) $Z_{HER2:342}$-SR-HP1 only. To evaluate the effect of non-targeted radiolabeled secondary agent, a control group 3 was injected with ^{177}Lu-HP2 (3.5 µg/16 MBq) only. In total this procedure was repeated six times, seven days between injections. The total injected radioactivity was 96 MBq per mouse.

To confirm tumor targeting, SPECT/CT imaging was performed. A group of five mice was imaged 30 h after injection of 16 MBq ^{177}Lu-HP2. Imaging was performed using nanoScan SC (Mediso Medical Imaging Systems, Hungary) under sevoflurane anesthesia. CT acquisitions were carried out using CT-energy peak of 50 keV, 670 µA, 480 projections, 2.3 min acquisition time. SPECT helical scans were acquired at the following parameters: ^{177}Lu energy window (50.49 keV – 61.71 keV, 101.61 keV – 124.19 keV, 187.56 keV – 229.24 keV), 110 projections, 256 × 256 matrix, 20 min acquisition time. CT raw files were reconstructed using Nucline 2.03 Software (Mediso Medical Imaging Systems, Hungary). SPECT raw data were reconstructed using Tera-Tomo™ 3D SPECT.

Histologic and Immunohistochemical Evaluation

The xenografts and kidneys from each mouse from the therapy experiment were formalin fixed and paraffin embedded using standard procedures. For histological evaluation 4 µm sections were stained with hematoxylin and eosin. To evaluate HER2 expression after experimental therapy, an immunohistochemical evaluation was performed using HercepTest Assay (Dako).

Statistical Analysis

GraphPad Prism software (GraphPad Software, Inc.) was used for statistical analysis. Biodistribution data were analyzed using 2-tail unpaired t-test to find significant differences ($p < 0.05$) when two groups were compared. When three or more groups were compared, a two-way ANOVA with Bonferroni test for multiple comparisons was applied. Survival data were analyzed using GraphPad Prism software.

RESULTS

Factors Influencing Pretargeting

The results of the experiments elucidating factors influencing pretargeting are presented in **Fig. 2**. The dosing and timing used in pretargeting of ^{111}In-HP2 (*23*) (**Fig. 2A**), resulted in the renal uptake higher than the tumor uptake. Co-injection of Gelofusine with ^{177}Lu-HP2 did not decrease the renal uptake. A doubling of ^{177}Lu-HP2-to- $Z_{HER2:342}$-SR-HP1 molar ratio by decreasing injected $Z_{HER2:342}$-SR-HP1 mass resulted in significant ($p<0.05$) reduction of the retention of activity in blood and the uptake in lung, liver and, most importantly, kidneys (**Fig.2 B**) while the tumor uptake of ^{177}Lu-HP2 had a tendency to increase. Increasing the interval between injections of $Z_{HER2:342}$-SR-HP1 and ^{177}Lu-HP2 from 4 to 8 h reduced significantly ($p<0.05$) the retention of activity in blood and the radioactivity uptake in lung, liver, spleen, and kidneys (**Fig. 2C**). The renal uptake after 16 h interval was significantly ($p<0.05$) lower than after 8 h. There was no significant difference between tumor uptake values when the interval between $Z_{HER2:342}$-SR-HP1 and ^{177}Lu-HP2 injections was 4, 8, or 16 h (**Fig. 2C**). Upscaling experiments (**Fig. 2D**) showed no significant changes in the biodistribution of ^{177}Lu-HP2, when the injected mass of both $Z_{HER2:342}$-SR-HP1 and ^{177}Lu-HP2 was doubled. Further a 1.5-fold increase of the ^{177}Lu-HP2 mass did not cause significant changes in tumor or kidney uptakes, but enabled an increase of the radioactivity delivered to tumors.

The tumor accumulation of ^{177}Lu-HP2 with no $Z_{HER2:342}$-SR-HP1 pre-injected was 0.2±0.1 %IA/g, which is significantly ($p<5\times10^{-5}$) lower than the accumulation after injection of any tested mass of $Z_{HER2:342}$-SR-HP1 at any tested time point. This suggests that the tumor uptake of ^{177}Lu-HP2 is dependent on affibody-directed PNA-mediated pretargeting.

Biodistribution and Dosimetry

Biodistribution and dosimetry data are presented in **Table 2**. Data demonstrate very rapid clearance of ^{177}Lu-HP2 from most tissues, e.g. the blood clearance proceeded with 13 (range 10-17) min half-life. The only tissues with prominent uptake were kidney and tumor. However, tumor uptake was four-fold higher than renal uptake already at 1 h after injection, as 84% of the renal uptake cleared with a 15 minute half-life, whereas the tumor clearance half-life was 63 h. Time integrated activity coefficient per gram of tissue for the tumor exceeded coefficients for kidneys, blood and bone 5.2-, 254- and 147-fold, respectively. Accordingly, the calculated mean absorbed dose to tumor was appreciably higher than the mean absorbed dose to any normal organ or tissue (**Table 2**).

Experimental Therapy

Imaging performed during experimental therapy (**Fig. 3**) demonstrated high accumulation of ^{177}Lu in tumors. Radioactivity concentration in kidneys was ca. 5-fold lower than in tumors, and concentration in other tissues was much lower.

The survival data are presented in **Fig. 4A**. The use of pretargeted therapy clearly improved survival of mice bearing HER2-expressing xenografts. The median survival in control groups was 32, 37, and 37 d for treatment with ^{177}Lu-HP2 alone, $Z_{HER2:342}$-SR-HP1 alone, or PBS, respectively. There was no significant difference between median survival times of animals in these groups. The median survival time of mice in the group treated with 16 MBq /3.5 µg ^{177}Lu-HP2 injected 16 h after injection of 100 µg (7.6 nmol) $Z_{HER2:342}$-SR-HP1 was 66 d, which was significantly ($p < 0.005$) longer than survival of mice in any of the control groups. One animal in this group, which had a tumor of 157 mm^3 at the therapy start, showed complete remission at day

61, which lasted until the end of the study (day 95). Detailed investigation of the body of this mouse did not reveal any visceral residual tumor or metastases. Absorbed dose to tumor was evaluated to be102 Gy.

The pretargeted therapy was well tolerated by mice. The appearance of skin, fat pads and eyes of treated mice did not differ from that of untreated healthy mice. There was no deviation of behavior indicating pain or suffering. The average animal weight was comparable to weights of mice injected with PBS (**Fig. 4B**).

Histologic and Immunohistochemical Evaluation

The evaluation of kidneys did not indicate any toxic impact by the treatment, there were well-preserved renal parenchymal structures, including glomeruli, tubuli and vessels (**Fig. 5).** Histological analysis of the xenografts showed a poorly differentiated cancer with solid morphology with variable areas of necrosis. The comparison of all four treatment groups did not reveal any difference in histological growth pattern or degree of necrosis (**Fig. 5**). Immunohistochemical analysis of the tumors demonstrated a moderate to strong membrane staining in almost all viable tumor cells (**Fig. 5**). The staining pattern revealed no difference in HER2 expression in the four treatment arms.

DISCUSSION

Pretargeting strategies have initially been created to overcome limitations associated with the bulkiness of immunoglobulin-based targeting vectors (*1*). We (*23*,*28*) and others (*29*) proposed to use pretargeting to compensate for undesirable high renal reabsorption of small targeting proteins. This study has demonstrated that pretargeting can be very efficient in reduction of renal uptake: at optimized conditions, renal uptake of ^{177}Lu-HP2 was 4±1 %IA/g at 4 p.i. This is 70-fold lower than the uptake of ^{177}Lu-labeled parental affibody molecules (*30*).

However, our study highlights some pitfalls in development of pretargeted therapies. For example, the renal uptake was higher than the tumor uptake (**Fig. 2A**) when we applied the same dosing and timing using ^{177}Lu-HP2, which provided higher uptake of ^{111}In-HP2 in tumor than in kidney (*23*). This was surprising since the data for ^{177}Lu-HP2 alone (*24*) demonstrated that renal uptake of ^{177}Lu-HP2 was not higher than uptake of ^{111}In-HP2. Furthermore, Gelofusine was not efficient for reduction of renal uptake in pretargeting settings (**Fig. 2A**) while it was efficient for ^{177}Lu-HP2 alone (*24*). On the other hand, Gelofusine does not reduce renal uptake of affibody molecules (*17*). This indicated that, most likely, ^{177}Lu-HP2 was taken up in kidneys as an adduct with $Z_{HER2:342}$-SR-HP1 formed by interaction with residual primary agent in blood. Reduction of the renal uptake after increase of the ^{177}Lu-HP2/ $Z_{HER2:342}$-SR-HP1 molar ratio confirmed this. The most efficient way to reduce the renal uptake was increasing the time between injection of primary and secondary probes, permitting sufficient clearance of $Z_{HER2:342}$-SR-HP1 (**Fig. 2C**). At optimized conditions, the PNA-mediated pretargeting provided more than five-fold higher absorbed dose to tumor compared with the absorbed dose to the kidneys. Earlier, we have evaluated another approach to affibody-based pretargeted therapy, the use of bioorthogonal reaction between trans-cyclooctene and tetrazine (*28*). In that case, the tumor absorbed dose

exceeded the renal absorbed dose approximately 1.4-fold at optimized conditions. Apparently, the use of PNA-PNA interaction provides much more favorable dosimetry for affibody-based pretargeting and is preferable.

Efficacy of pretargeted therapy has been demonstrated in this study by significant extension of survival. No pathologic changes in kidneys were observed (**Fig. 5**). This is in agreement with the current practice of clinical radionuclide therapy, which is given with palliative intent. Increase of absorbed dose rate should increase efficacy of tumor treatment. This might be achieved by the use of no-carrier-added ^{177}Lu or the use of alpha-emitting ^{225}Ac.

It has to be noted that our approach could be easily applied to other ESPs. The use of an optimized protocol (*24*) should provide efficient ligation of hybridization probes to any ESP containing an LPXTG-tag. This might enable development of pretargeted radionuclide therapy based on ESPs having high renal reabsorption, such as fibronectin domains. In all cases, site-specific coupling of HP1 would provide well-defined homogenous constructs with reproducible biodistribution.

CONCLUSION

Optimizing of timing and dosing of injection of affibody molecules containing a PNA-based hybridization probe and a ^{177}Lu-labeled complementary probe enabled delivery of absorbed dose to tumors that exceeded absorbed doses to kidneys. Affibody-based PNA-mediated pretargeted radionuclide therapy increased significantly the survival of mice bearing human HER2-expressing cancer xenografts.

ACKNOWLEDGEMENTS

This research was financially supported by grants from the Swedish Cancer Society, the Swedish Research Council, ProNova VINN Excellence Centre for Protein Technology and the Swedish Agency for Innovation VINNOVA.

REFERENCES

1. Stoldt HS, Aftab F, Chinol M, et al. Pretargeting strategies for radio-immunoguided tumour localisation and therapy. *Eur J Cancer*. 1997;33:186-92.

2. Pouget JP, Navarro-Teulon I, Bardiès M, et al. A clinical radioimmunotherapy--the role of radiobiology. *Nat Rev Clin Oncol*. 2011;8:720-734.

3. van de Watering FC, Rijpkema M, Robillard M, Oyen WJ, Boerman OC. Pretargeted imaging and radioimmunotherapy of cancer using antibodies and bioorthogonal chemistry. *Front Med (Lausanne)*. 2014;1:44.

4. Altai M, Membreno R, Cook B, Tolmachev V, Zeglis BM. A primer on pretargeted imaging and therapy. *J Nucl Med*. 2017;58:1553-1559.

5. Vazquez-Lombardi R, Phan TG, Zimmermann C, Lowe D, Jermutus L, Christ D. Challenges and opportunities for non-antibody scaffold drugs. *Drug Discov Today*. 2015;20:1271-1283.

6. Stern LA, Case BA, Hackel BJ. Alternative non-antibody protein scaffolds for molecular imaging of cancer. *Curr Opin Chem Eng*. 2013;2:425–432.

7. Feldwisch J, Tolmachev V. Engineering of affibody molecules for therapy and diagnostics. *Methods Mol Biol*. 2012;899:103-126.

8. Hackel BJ, Kimura RH, Gambhir SS. Use of 64Cu-labeled fibronectin domain with EGFR-overexpressing tumor xenograft: molecular imaging. *Radiology*. 2012; 263:179-188.

9. Goldstein R, Sosabowski J, Livanos M, et al. Development of the designed ankyrin repeat protein (DARPin) G3 for HER2 molecular imaging. *Eur J Nucl Med Mol Imaging*. 2015;42:288-301.

10. Garousi J, Lindbo S, Nilvebrant J, et al. ADAPT, a novel scaffold protein-based probe for radionuclide imaging of molecular targets that are expressed in disseminated cancers. *Cancer Res*. 2015;75:4364-4371.

11. Nord K, Gunneriusson E, Ringdahl J, Ståhl S, Uhlén M, Nygren PA. Binding proteins selected from combinatorial libraries of an alpha-helical bacterial receptor domain. *Nat Biotechnol*. 1997;15:772-777.

12. Ståhl S, Gräslund T, Eriksson Karlström A, Frejd FY, Nygren PÅ, Löfblom J. Affibody molecules in biotechnological and medical applications. *Trends Biotechnol*. 2017;35:691-712.

13. Bartley AN, Washington MK, Colasacco C, et al. HER2 testing and clinical decision making in gastroesophageal adenocarcinoma: guideline from the college of American Pathologists, American Society for Clinical Pathology, and the American Society of Clinical Oncology. *J Clin Oncol*. 2017;35:446-464.

14. Wolff AC, Hammond ME, Hicks DG, et al. Recommendations for human epidermal growth factor receptor 2 testing in breast cancer: American Society of Clinical Oncology/College of American Pathologists clinical practice guideline update. *J Clin Oncol*. 2013;31:3997-4013.

15. Sörensen J, Sandberg D, Sandström M, et al. First-in-human molecular imaging of HER2 expression in breast cancer metastases using the ^{111}In-ABY-025 affibody molecule. *J Nucl Med*. 2014;55:730-735.

16. Sörensen J, Velikyan I, Sandberg D, et al. Measuring HER2-receptor expression in metastatic breast cancer using [^{68}Ga]ABY-025 affibody PET/CT. *Theranostics*. 2016;6:262-271.

17. Altai M, Varasteh Z, Andersson K, Eek A, Boerman O, Orlova A. In vivo and in vitro studies on renal uptake of radiolabeled affibody molecules for imaging of HER2 expression in tumors. *Cancer Biother Radiopharm*. 2013;28:187-195.

18. Egholm M, Buchardt O, Christensen L, et al. PNA hybridizes to complementary oligonucleotides obeying the Watson-Crick hydrogen-bonding rules. *Nature*. 1993;365:566–568.

19. Cutrona G, Boffa LC, Mariani MR, et al. The peptide nucleic acid targeted to a regulatory sequence of the translocated c-myc oncogene in Burkitt's lymphoma lacks immunogenicity: follow-up characterization of PNAEmu-NLS. *Oligonucleotides*. 2007;17:146–150.

20. Boffa LC, Menichini P, Bolognesi C, et al. Lack of mutagenicity and clastogenicity of Emu-NLS targeted to a regulatory sequence of the translocated c-myc oncogene in Burkitt's lymphoma. *Mutat Res*. 2007;628:129–137.

21. Rusckowski M, Qu T, Chang F, Hnatowich DJ. Pretargeting using peptide nucleic acid. *Cancer*. 1997;80:2699–2705.

22. Westerlund K, Honarvar H, Tolmachev V, Eriksson Karlström A. Design, preparation, and characterization of PNA-based hybridization probes for affibody-molecule-mediated pretargeting. *Bioconjug Chem*. 2015;26:1724-1736.

23. Honarvar H, Westerlund K, Altai M, et al. Feasibility of affibody molecule-based PNA-mediated radionuclide pretargeting of malignant tumors. *Theranostics.* 2016;6:93-103.

24. Altai M, Westerlund K, Velletta J, Mitran B, Honarvar H, Eriksson Karlström A. Evaluation of affibody molecule-based PNA-mediated radionuclide pretargeting: development of an optimized conjugation protocol and ^{177}Lu labeling. *Nucl Med Biol*. 2017;54:1-9.

25. Rolleman EJ, Melis M, Valkema R, Boerman OC, Krenning EP, de Jong M. Kidney protection during peptide receptor radionuclide therapy with somatostatin analogues. *Eur J Nucl Med Mol Imaging*. 2010;37:1018-31.

26. Keenan MA, Stabin MG, Segars WP, Fernald MJ. RADAR realistic animal model series for dose assessment. *J Nucl Med*. 2010;5:471-476.

27. Stabin MG, Konijnenberg MW. Re-evaluation of absorbed fractions for photons and electrons in spheres of various sizes. *J Nucl Med*. 2000;41:149-160.

28. Altai M, Perols A, Tsourma M, et al. Feasibility of affibody-based bioorthogonal chemistry-mediated radionuclide pretargeting. *J Nucl Med*. 2016;57:431-436.

29. van Duijnhoven SM, Rossin R, van den Bosch SM, Wheatcroft MP, Hudson PJ, Robillard MS. Diabody pretargeting with click chemistry in vivo. *J Nucl Med*. 2015;56:1422-1428.

30. Fortin MA, Orlova A, Malmström PU, Tolmachev V. Labelling chemistry and characterization of [$^{90Y/177}$Lu]-DOTA-ZHER2:342-3 Affibody molecule, a candidate agent for locoregional treatment of urinary bladder carcinoma. *Int J Mol Med*. 2007;19:285-291.

FIGURES CAPTIONS

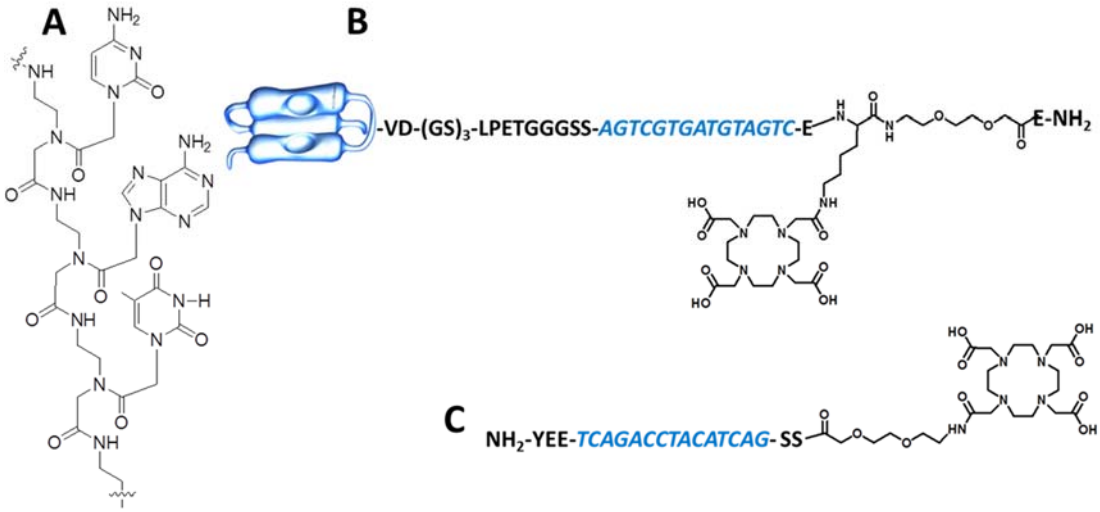

FIGURE 1. A. An example of a PNA structure; B. HP1 hybridization probe ligated to an affibody molecule (ZHER2:342-SR-HP1) and DOTA; C. HP2 complementary hybridization probe with DOTA. One-letter codes are applied for designation of both amino acid and nitrogenous bases. The PNA part is marked in blue Italic.

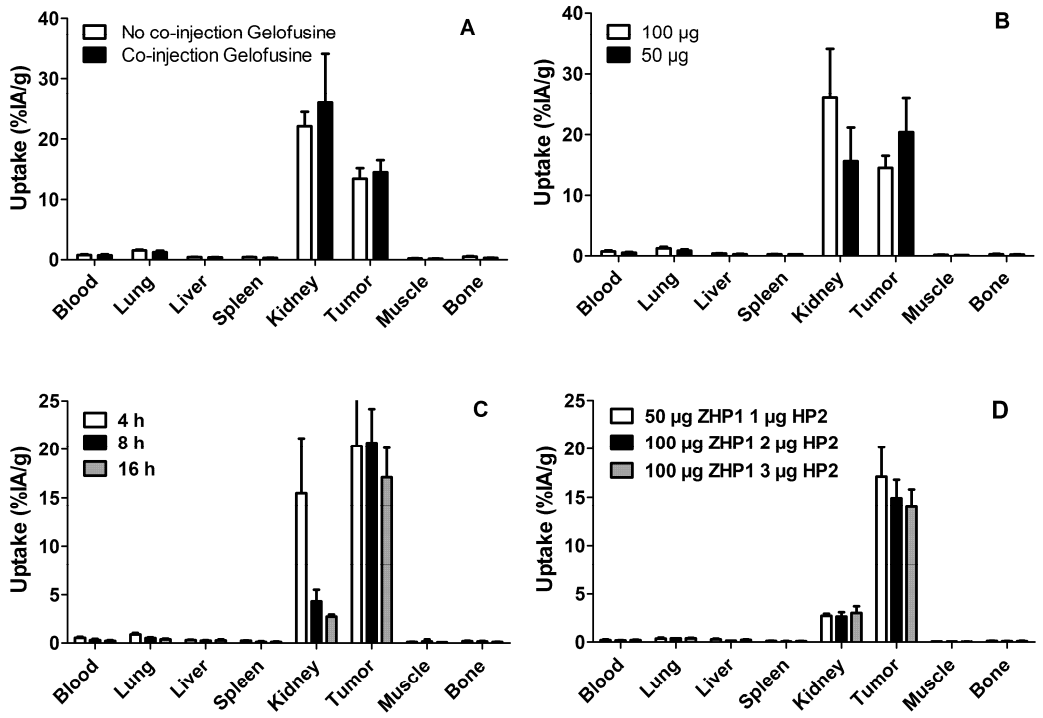

FIGURE 2. Factors influencing pretargeting. All biodistribution measurements were performed 1 h after injection of ^{177}Lu-HP2. **A**. Gelofusine effect on renal uptake. Mice were injected with 100 µg $Z_{HER2:342}$-SR-HP1, 4 h later 1 µg ^{177}Lu-HP2 was injected. In one group, 4 mg Gelofusine was co-injected with ^{177}Lu-HP2. **B.** Influence of ^{177}Lu-HP2/ZHP1 molar ratio. Mice were injected with 50 or 100 µg $Z_{HER2:342}$-SR-HP1, 4 h later 1 µg ^{177}Lu-HP2 was injected. **C**. Influence of time between injections of primary and secondary agents. 1 µg ^{177}Lu-HP2 was injected after 4, 8 or 16 h after injection of 50 µg $Z_{HER2:342}$-SR-HP1. **D.** Increasing the quantity of injected ^{177}Lu-HP2. 2 and 3 µg ^{177}Lu-HP2 was injected at 16 h after injection of 100 µg $Z_{HER2:342}$-SR-HP1.

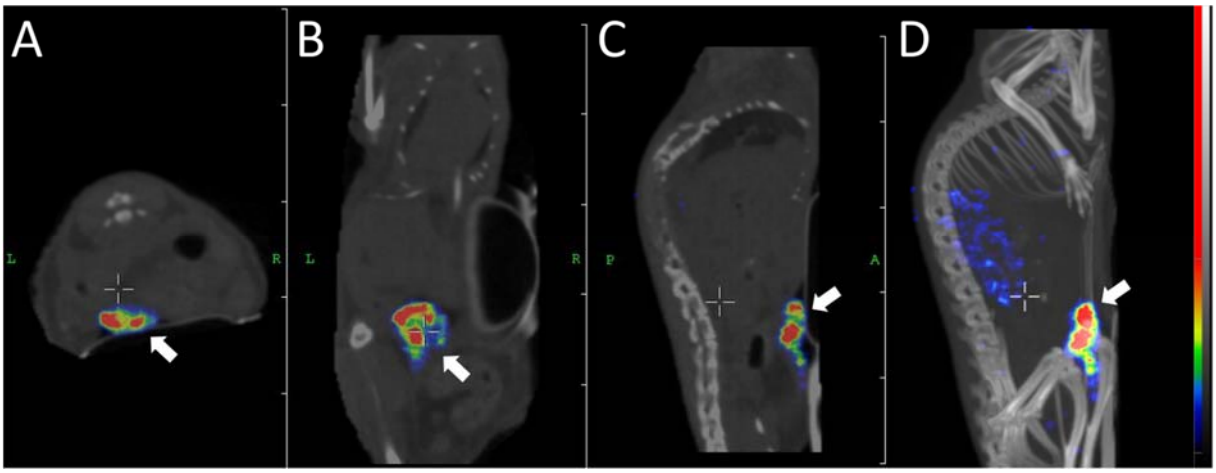

FIGURE 3. Transversal (A), coronal (B), sagittal (C) nanoSPECT/CT images and maximum intensity projection (D) obtained 30 h after injection of pretargeted ^{177}Lu-HP2. Tumor (indicated by arrow) was located on the abdomen.

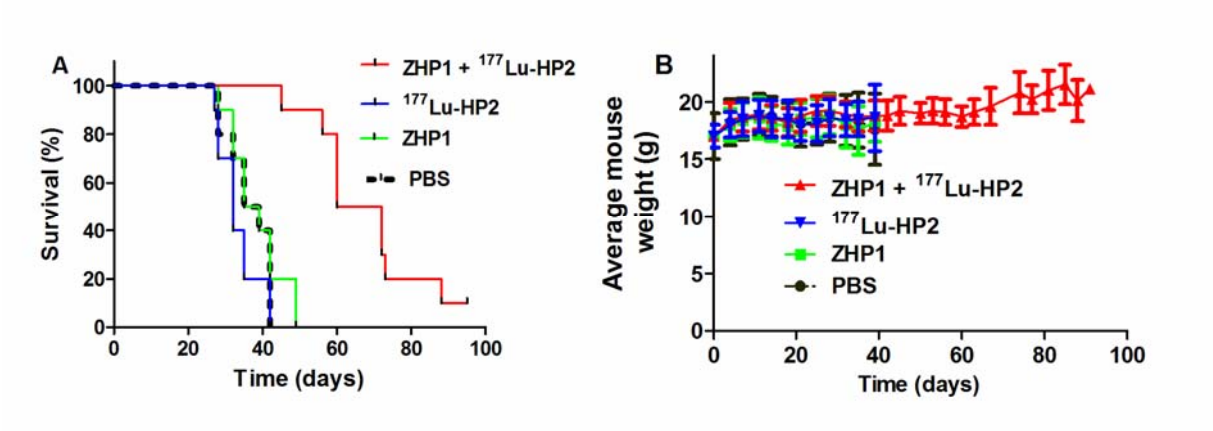

FIGURE 4. Survival of BALB/C nu/nu mice treated with $Z_{HER2:342}$-SR-HP1/^{177}Lu-HP2, ^{177}Lu-HP2 alone, $Z_{HER2:342}$-SR-HP1 alone or PBS alone (A) and average animal weight during therapy (B).

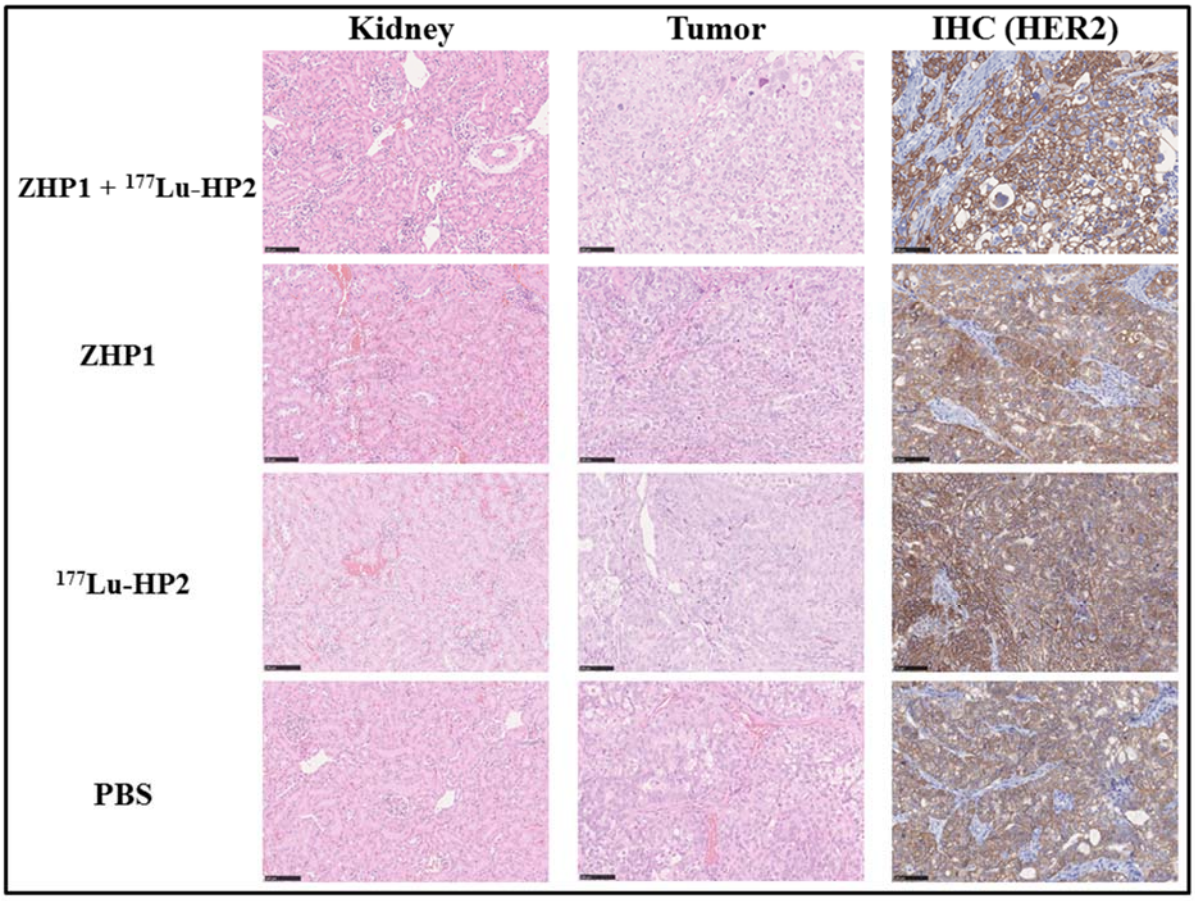

FIGURE 5. Representative images of hematoxylin and eosin staining of kidneys cortical region (left column) and tumor (middle column) and immunohistochemical analysis of HER2-expression in tumor (right column) for mice treated using pretargeting.

TABLE 1. Parameters evaluated during optimization of pretargeting.

Injected mass of ZHER2:342-SR-HP1 (μg)/(nmol)	Injected mass of ^{177}Lu-HP2 (μg)/(nmol)	Time between injection of ZHER2:342-SR-HP1 and ^{177}Lu-HP2 (h)	Co-injection of Gelofusine with ^{177}Lu-HP2
100/7.6	1/0.19	4	no
100/7.6	1/0.19	4	yes
50/3.8	1/0.19	4	yes
50/3.8	1/0.19	8	yes
50/3.8	1/0.19	16	yes
no	1/0.19	-	yes
100/7.6	2/0.38	16	yes
100/7.6	3/0.57	16	yes

TABLE 2. Biodistribution and dosimetry of ^{177}Lu-HP2 injected 16 h after $Z_{HER2:342}$-SR-HP1 in Balb/C nu/nu mice bearing SKOV-3 xenografts.

	Uptake (%IA/g)							Estimated mean absorbed dose (mGy/MBq)
	0.3 h	1 h	4 h	24 h	48 h	144 h	216 h	
Blood	2.2±0.3	0.28±0.07	0.019±0.003	0.010±0.005	0.008±0.001			4.0
Heart	0.8±0.1	0.12±0.06	0.03±0.01	0.016±0.007	0.02±0.02			5.4
Lung	1.9±0.2	0.41±0.07	0.15±0.01	0.06±0.01	0.05±0.01			14.4
Salivary glands	0.9±0.2	0.2±0.1	0.06±0.02	0.04±0.01	0.03±0.01			9.3
Liver	0.56±0.06	0.20±0.02	0.15±0.04	0.12±0.03	0.11±0.05	0.06±0.03	0.05±0.02	13.3
Spleen	0.59±0.08	0.14±0.03	0.07±0.02	0.08±0.02	0.06±0.01			12.8
Pancreas	0.5±0.2	0.10±0.02	0.024±0.007	0.017±0.008	0.02±0.01			4.0
Stomach	1.1±0.2	0.19±0.03	0.10±0.03	0.05±0.03	0.033±0.006			12.3
Small intestine	0.7±0.1	0.14±0.02	0.05±0.02	0.03±0.02	0.027±0.007			7.0
Large intestine	0.9±0.3	0.18±0.03	0.07±0.03	0.03±0.02	0.05±0.02			10.4
Kidney	12±2	5±1	4±1	3±1	2.3±0.7	0.7±0.2	0.5±0.2	205.6
Kidney cortex*								267
Tumor	15±3	20±5	17±3	15±2	12±1	3.4±0.6	1.8±0.3	1075.4
Skin	1.8±0.3	0.3±0.1	0.13±0.03	0.10±0.05	0.08±0.03	0.03±0.01	0.04±0.02	
Muscle	0.6±0.1	0.10±0.04	0.03±0.01	0.014±0.003	0.019±0.008			
Bone	0.64±0.07	0.13±0.04	0.04±0.01	0.03±0.01	0.03±0.01			6.8
Brain	0.07±0.01	0.01±0.00	0.004±0.002	0.002±0.002	0.002±0.001			0.6

Biodistribution data are presented as an average %IA/g ± SD (n = 5).

* Estimated based on autoradiography data.

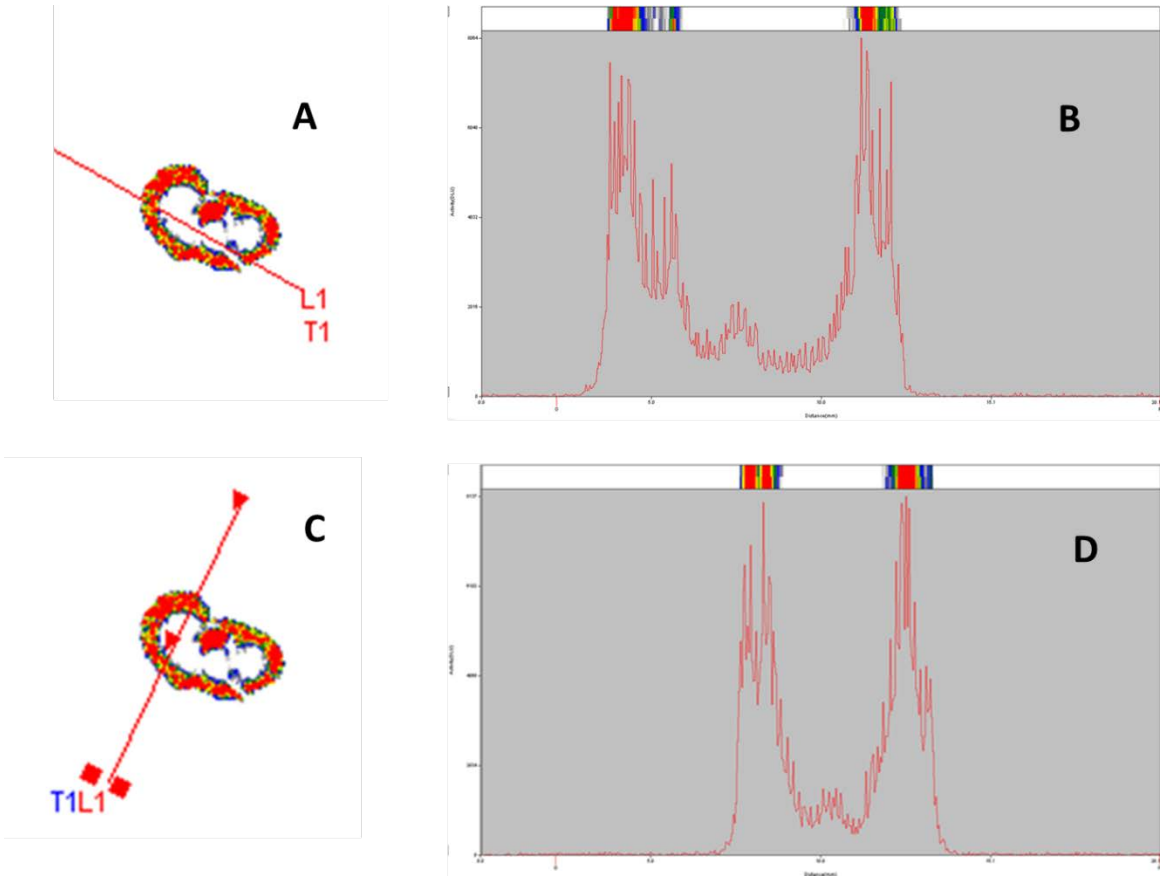

Supplemental Fig.1 Evaluation of distribution of ^{177}Lu-HP2 in kidneys. Two BALB/C nu/nu mice were injected with 100 µg (7.6 nmol) $Z_{HER2:342}$-SR-HP1 each. ^{177}Lu-HP2, 3 µg (1 MBq) per mouse, was injected 16 h later. Animals were sacrificed 1 h after injection of ^{177}Lu-HP2. Kidneys were excised and 20 µm-cryosections were prepared. Distribution of radioactivity in the sections was measured by digital autoradiography using a Cyclone Storage Phosphor System (PerkinElmer). (A) and (C) show digital autoradiography of a kidney. (B) and (C) show distribution of radioactivity along the lines marked in /A) and (C), respectively.

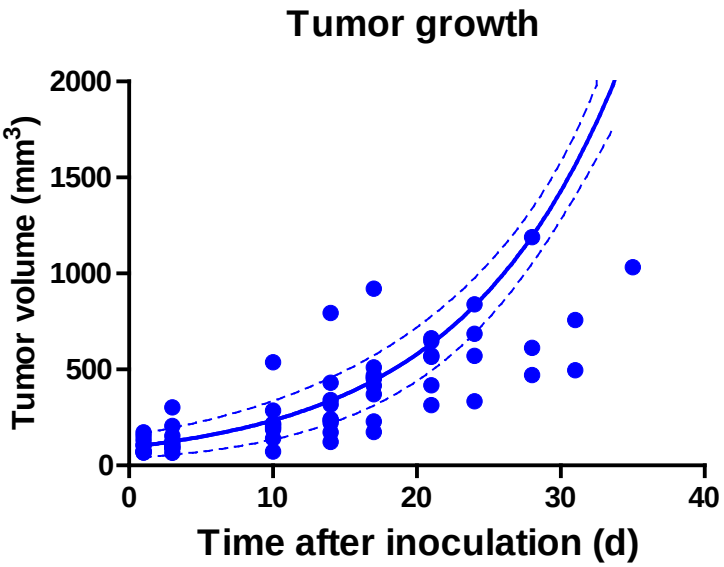

Supplemental Fig.2 SKOV-3 xenograft growth data, which were used for calculations of absorbed doses to tumors.